[2] D. W. Tufts and R. Kumaresan, "Estimation of multiple sinusoids: making linear prediction perform like maximum likelihood," *Proc. IEEE*, vol. 70, pp. 975–989, Sept. 1982.
[3] K. Nishiyama, "A nonlinear filter for estimating a sinusoidal signal and its parameters in white noise: On the case of a single sinusoid," *IEEE Trans. Signal Processing*, vol. 45, pp. 970–981, Apr. 1997.
[4] S. Kay, "A fast and accurate single frequency estimator," *IEEE Trans. Acoust., Speech, Signal Processing*, vol. 37, pp. 1987–1990, Dec. 1989.
[5] P. M. Djuric and S. M. Kay, "Parameter estimation of chirp signals," *IEEE Trans. Acoust., Speech, Signal Processing*, vol. 38, pp. 2118–2126, Dec. 1990.
[6] D. Kim, M. J. Narasimha, and D. C. Cox, "An improved single frequency estimator," *IEEE Signal Processing Lett.*, vol. 3, pp. 212–214, July 1996.
[7] G. W. Lank, I. S. Reed, and G. E. Pollon, "A semicoherent detection and Doppler estimation statistic," *IEEE Trans. Aerosp. Electron. Syst.*, vol. AES-9, pp. 151–165, Mar. 1973.
[8] S. Umesh and D. Nelson, "Computationally efficient estimation of sinusoidal frequency at low SNR," in *Proc. IEEE Int. Conf. Acoust., Speech, Signal Process.*, 1996, pp. 2797–2800.
[9] M. Vetterli and J. Kovačević, *Wavelets and Subband Coding.* Englewood Cliffs, NJ: Prentice-Hall, 1995.

Cross-Product Algorithms for Source Tracking Using an EM Vector Sensor

Arye Nehorai and Petr Tichavský

***Abstract*—We present an adaptive cross-product algorithm for tracking the direction to a moving source using an electromagnetic vector sensor and analyze its performance. We then propose a multiple forgetting factor variant of the same algorithm, which has self-tuning capability. Numerical examples are included.**

***Index Terms*—Array processing, tracking algorithms, vector sensor.**

I. Introduction

In this correspondence, we develop adaptive cross-product algorithms for tracking the direction to an electromagnetic (EM) source. These algorithms use measurements from an EM vector sensor (a device measuring the complete six components of an EM field at a single point). They extend the original method for stationary sources in [1] and [2]. Comparison of the method with a conventional array processing is a subject of [3].

Inspired by the Poynting theorem, the method in [1] and [2] forms the cross-product of the electric field vector with the complex conjugate of the magnetic field vector and averages it over time. The vector result is normalized to have unit length, yielding the estimate of the unit vector in the source direction. The resulting cross-product algorithm has no scalar-sensor counterpart. Its principal advantages and capabilities are the following:

- very low computational complexity since no cost function minimization is needed;
- ability to easily and equally work with sources of various types, such as wideband or narrowband signals, polarized or unpolarized.

The ability to work with wideband sources with low computational complexity occurs because the steering vector is not a function of the frequency. Other advantages that are inherited by the properties of the vector sensor are as follows.

- Only one EM vector sensor is needed to track the source in three-dimensional (3-D) space while occupying very little space.
- There is no need for sensor location calibration and time synchronization among different components since no time delays are used.
- There is isotropic response.

The correspondence is organized as follows. In Section II, we introduce and analyze the simplest form of the adaptive cross-product algorithm in which a forgetting factor is used to discount old data measurements in the averaging. For its performance analysis, a most difficult tracking scenario is considered where the signal angle of arrival has independent random Gaussian distributed increments. In Section III, we present another version of the algorithm that is of the multiple forgetting factor (MFF) type. It is fully adaptive in the sense that it has a nearly optimum performance in scenarios with unknown or time-varying signal-to-noise ratio (SNR) and rate of changes of the angle of the wave arrival. In Section IV, we illustrate the performance of the proposed algorithms via numerical examples. Section V summarizes our conclusions.

II. Adaptive Cross-Product Algorithm

The cross-product algorithm for estimating the direction to a far-field source is based on the fact that in an electromagnetic plane wave, the instantaneous vectors of the electric and magnetic fields and the direction vector of wave propagation are mutually orthogonal. Thus, if the former two vectors are measured by a six-component vector sensor, the direction of the wave can be found by computing the cross product of these vectors.

Since, in general, the measurements are noisy and the signal is nonstationary, we propose to estimate the instantaneous vector of direction of the wave as a weighted average of the sequence of the individual cross products using an exponential window with a forgetting factor λ

$$\hat{\boldsymbol{s}}_N = \frac{1}{\sum_{t=1}^{N} \lambda^{-t}} \sum_{t=1}^{N} \lambda^{-t}\, \mathrm{Re}\{\boldsymbol{y}_{\mathrm{E}}(t) \times \overline{\boldsymbol{y}}_{\mathrm{H}}(t)\} \tag{1}$$

$$\hat{\boldsymbol{u}}_N = \hat{\boldsymbol{s}}_N / ||\hat{\boldsymbol{s}}_N||. \tag{2}$$

In (1), $\boldsymbol{y}_{\mathrm{E}}(t)$ is the 3-D electric field measurement and $\overline{\boldsymbol{y}}_{\mathrm{H}}(t)$ the complex conjugate of the 3-D magnetic field measurement in phasor (complex envelope) form.

Let $\boldsymbol{e}_{\mathrm{E}}(t)$ and $\boldsymbol{e}_{\mathrm{H}}(t)$ be errors (additive noise) that enter the measurements of the electric and magnetic fields $\boldsymbol{y}_{\mathrm{E}}(t)$ and $\boldsymbol{y}_{\mathrm{H}}(t)$. As in [2], we assume that these errors are zero mean, independent of each

Manuscript received July 16, 1998; revised April, 2, 1999. This work was supported by the Air Force Office of Scientific Research under Grants F49620-97-1-0481 and F49620-99-1-0067, the National Science Foundation under Grant MIP-9615590, the Office of Naval Research under Grant N00014-98-1-0542, and the Grant Agency of the Czech Republic through Grant 102/97/0466. The associate editor coordinating the review of this paper and approving it for publication was Dr. Jean Jacques Fuchs.

A. Nehorai is with Department of Electrical Engineering and Computer Science, University of Illinois at Chicago, Chicago, IL 60607-7053 USA.

P. Tichavský is with the Institute of Information Theory and Automation, Academy of Sciences of the Czech Republic, Prague, Czech Republic.

Publisher Item Identifier S 1053-587X(99)07697-7.

other and of the signal itself, and have the following covariances:

$$\mathrm{E}\begin{bmatrix} \boldsymbol{e}_{\mathrm{E}}(t) \\ \boldsymbol{e}_{\mathrm{H}}(t) \end{bmatrix} [\overline{\boldsymbol{e}}_{\mathrm{E}}^{T}(s), \quad \overline{\boldsymbol{e}}_{\mathrm{H}}^{T}(s)] = \begin{bmatrix} \sigma_{\mathrm{E}}^2 I_3 & 0 \\ 0 & \sigma_{\mathrm{H}}^2 I_3 \end{bmatrix} \tag{3}$$

$$\mathrm{E}\begin{bmatrix} \boldsymbol{e}_{\mathrm{E}}(t) \\ \boldsymbol{e}_{\mathrm{H}}(t) \end{bmatrix} [\boldsymbol{e}_{\mathrm{E}}^{T}(s), \boldsymbol{e}_{\mathrm{H}}^{T}(s)] = 0 \quad \text{(for all } t \text{ and } s). \tag{4}$$

The superscript "T" denotes the transpose and I_3 the 3-D identity matrix. In [2], it was shown that the term $\hat{z}_t \triangleq \mathrm{Re}\{\boldsymbol{y}_{\mathrm{E}}(t) \times \overline{\boldsymbol{y}}_{\mathrm{H}}(t)\}$ can be written as $\hat{z}_t = z_t + \delta \boldsymbol{z}_t$, where z_t is a deterministic part proportional to the true source direction vector, $\boldsymbol{z}_t = \sigma_s^2 \cdot \boldsymbol{u}_t$, and $\sigma_s^2 = \mathrm{E}[|s(t)|^2]$ is the variance of the complex envelope of the (scalar) transmitted signal $s(t)$. Stochastic properties of the error term $\delta \boldsymbol{z}_t$ were studied in [2].

For analyzing the tracking, we consider a worst-case model of $\boldsymbol{u}_t$

$$\boldsymbol{u}_{t+1} = \frac{\boldsymbol{u}_t + \boldsymbol{n}_t}{||\boldsymbol{u}_t + \boldsymbol{n}_t||} \tag{5}$$

where $\{\boldsymbol{n}_t\}$ are independent samples from the distribution $\mathcal{N}(0, \sigma_n^2 I_3)$. Thus, the source moves randomly and equally likely in all directions from its position at the previous time sample. In the Appendix, we approximate the variance of the angular estimation error $\delta\varphi_t$ (between the source direction and its estimate) as

$$\mathrm{var}[\delta\varphi_t] = \frac{1-\lambda}{1+\lambda}\sigma_x^2 + \frac{2\lambda^2}{1-\lambda^2}\sigma_n^2 + O(\mathrm{E}[||\delta \boldsymbol{z}_t||^3]\sigma_s^{-6} + \sigma_n^3) \tag{6}$$

where

$$\sigma_x^2 = \frac{\sigma_{\mathrm{E}}^2 + \sigma_{\mathrm{H}}^2}{2\sigma_s^2} + \frac{2\sigma_{\mathrm{E}}^2\sigma_{\mathrm{H}}^2}{\sigma_s^4}. \tag{7}$$

We now use the above result to compute an optimal value of the forgetting factor. If the remainder term in (6) is neglected, the leading term in the equation is minimized for

$$\lambda = \lambda_0 \triangleq 1 + \kappa - \sqrt{2\kappa + \kappa^2} \tag{8}$$

where

$$\kappa = \frac{\sigma_n^2}{\sigma_x^2}. \tag{9}$$

The Taylor series expansion of (8) gives

$$\lambda_0 = \begin{cases} 1 - \sqrt{2\kappa} + O(\kappa), & \text{for } \kappa \to 0 \\ \dfrac{1}{2\kappa} + O\left(\dfrac{1}{\kappa^2}\right), & \text{for } \kappa \to \infty. \end{cases} \tag{10}$$

This optimal choice of λ is a tradeoff between system responsiveness and noise sensitivity. The source position fluctuates with amplitude that increases with σ_n; therefore, when σ_n^2 is large, we expect a smaller forgetting factor to yield better performance. A smaller forgetting factor lets old data samples be "forgotten" more quickly. However, as with other tracking systems, a responsive system is generally more susceptible to measurement noise since time averages are generally short, whereas a noise tolerant system is not able to follow rapid movement of the source. Hence, a tradeoff between these conflicting performance measures is needed and is solved by λ_0.

III. Multiple Forgetting Factor Algorithm

The performance of the tracking algorithm in (1)–(2) depends on the forgetting factor λ. Achieving an optimum performance of the algorithms is possible only if time dynamic properties of the system are known. If this *a priori* information is missing, we suggest the use of the *multiple forgetting factor* technique proposed by Uosaki *et al.* [5]. This technique consists of combining a number M (usually $M = 3$) estimates obtained by multiple applications of the same algorithm in parallel with constant but different forgetting factors.

Let $\hat{\boldsymbol{u}}_t^{(i)}$, $i = 1, \cdots, M$ denote the estimates of the direction vector $\boldsymbol{u}_t$ obtained by the algorithm with forgetting factors $\lambda_1, \cdots, \lambda_M$ such that $1 > \lambda_1 > \cdots > \lambda_M > 0$ by processing data up to time t. The combined estimate is given as a weighted average

$$\hat{\boldsymbol{u}}_t = \sum_{i=1}^{M} w^{(i)} \hat{\boldsymbol{u}}_t^{(i)} \tag{11}$$

where

$$w^{(i)} = \frac{w_{t-W}^{(i)} \prod_{k=t-W+1}^{t} p(y^k|i)}{\sum_{j=1}^{M} w_{t-W}^{(j)} \prod_{k=t-W+1}^{t} p(y^k|j)} \tag{12}$$

$$w_{t-W}^{(i)} = 1/M \tag{13}$$

$$p(y^t|i) = \frac{1}{\sqrt{2\pi}\hat{\sigma}_t} \exp\left\{-\frac{[y_t - \hat{y}_{t-1}^{(i)}]^2}{2\hat{\sigma}_t^2}\right\} \tag{14}$$

$$\hat{\sigma}_t^2 = \sum_{i=1}^{M} w^{(i)} \hat{\sigma}_t^{(i)2} \tag{15}$$

$$\hat{\sigma}_t^{(i)2} = \lambda_i \hat{\sigma}_{t-1}^{(i)2} + (1 - \lambda_i)[y_t - \hat{y}_{t-1}^{(i)}]^2. \tag{16}$$

In (12), W is the integer part of the median of $1/(1-\lambda_i)$, $i = 1, \cdots, M$. In the general technique proposed in [5], the term $\hat{y}_{t-1}^{(i)}$ in (14) and (16) is replaced by a more general one-step-ahead prediction of y_t based on the data $\{y_k; k < t\}$.

An advantage of the MFF technique is that it does not require that the choice of λ be taken care of as in the original algorithm, i.e., this modified algorithm has a self tuning ability. On the other hand, it has a higher computational complexity.

IV. Simulations

Example 1—Tracking Randomly Moving Source: We generated a sequence of unit vectors $\{\boldsymbol{u}_t\}_{t=1}^{500}$ recursively using (5) starting with $\boldsymbol{u}_0 = [0, 0, 1]^T$, and $\{\boldsymbol{n}_t\}$ are independent and identically distributed according to $\mathcal{N}(0, \sigma_n^2 I_3)$ with $\sigma_n = 0.005$. Since the one-step source angular movement is $\Delta\varphi_t \triangleq 2 \arcsin(||\boldsymbol{u}_t - \boldsymbol{u}_{t-1}||/2) \approx ||\boldsymbol{u}_t - \boldsymbol{u}_{t-1}|| \approx ||(I_3 - \boldsymbol{u}_t\boldsymbol{u}_t^T)\boldsymbol{n}_t||$ [cf. (21)], its expected value is $\mathrm{E}[\Delta\varphi_t] \approx \sqrt{\pi/2}\sigma_n \approx 6.3 \cdot 10^{-3}$[rad] ≈ 0.36[deg]. Measurements are obtained as $\hat{z}_t = \boldsymbol{u}_t + \delta \boldsymbol{z}_t$, $t = 1, \cdots, N$, where $\delta \boldsymbol{z}_t$ is a sequence of independent $\mathcal{N}(0, 10^{-2} I_3)$-distributed vectors; see also the Appendix. This choice corresponds to $\sigma_s^2 = 1$ and $\sigma_{\mathrm{E}}^2 = \sigma_{\mathrm{H}}^2 = 0.01$. The first component of the data $\hat{z}_t$ is plotted in the top diagram of Fig. 1.

The data are processed by the algorithm described in (1) and (2) for the optimum parameter $\lambda = \lambda_0 = 0.9317$ obtained from (8). The true and estimated first component of $\{\boldsymbol{u}_t\}_{t=1}^{500}$ are marked by dashed and full lines, respectively, in the middle diagram in Fig. 1. The bottom diagram shows the angular error of the estimate.

Example 2—Tracking by MFF Technique: In this example, the sequence $\{\boldsymbol{u}_t\}_{t=1}^{500}$ is taken to be deterministic. It is constant and equal to $[1, 1, 0]/\sqrt{2}$ in the time intervals (1, 150) and (350, 500), whereas in the interval (150, 350), the direction vector draws a circle with the center at $[1, 1, 1/2] \cdot 2/3$. In this interval, the angular velocity is 0.612 deg./iteration. The data are embedded in the same additive noise as in the previous examples. Results for the basic cross-product algorithm with $\lambda = 0.9$ and $\lambda = 0.97$ are shown in Figs. 2 and 3, respectively. Results for the MFF technique with forgetting factors 0.85, 0.97, 0.995 are shown in Fig. 4.

We can see that the MFF technique is almost as capable to suppress the noise as the original algorithm with $\lambda = 0.97$ when the data are

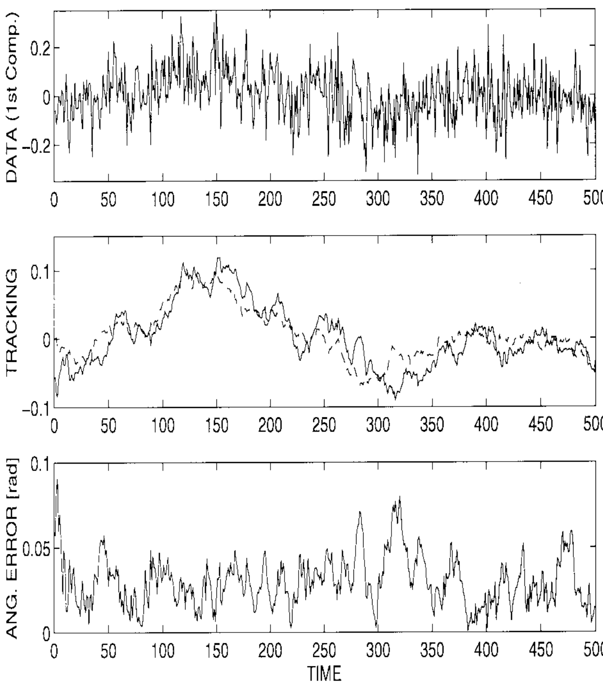

Fig. 1. Performance of the adaptive cross-product algorithm with optimum forgetting factor in the worst-case scenario. Top diagram: noisy data (first component of $\hat{z}_t$). Middle diagram: true and estimated first component denoted by dashed and full lines, respectively. Bottom diagram: angular estimation error.

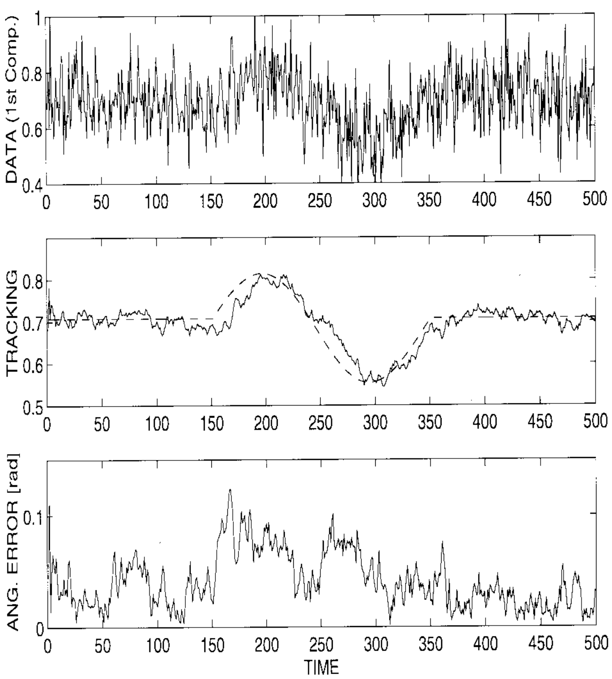

Fig. 2. Performance of the cross-product algorithm with $\lambda = 0.9$. Top diagram: noisy data (first component of $\hat{z}_t$). Middle diagram: true and estimated first component denoted by dashed and full lines, respectively. Bottom diagram: angular estimation error.

stationary and almost as well track the signal when it is nonstationary as the algorithm with $\lambda = 0.9$. The number of flops (floating point operations counted by Matlab) was about 12 times higher than those of the original algorithm with a fixed λ. In particular, it was 265k flops compared with 21k flops.

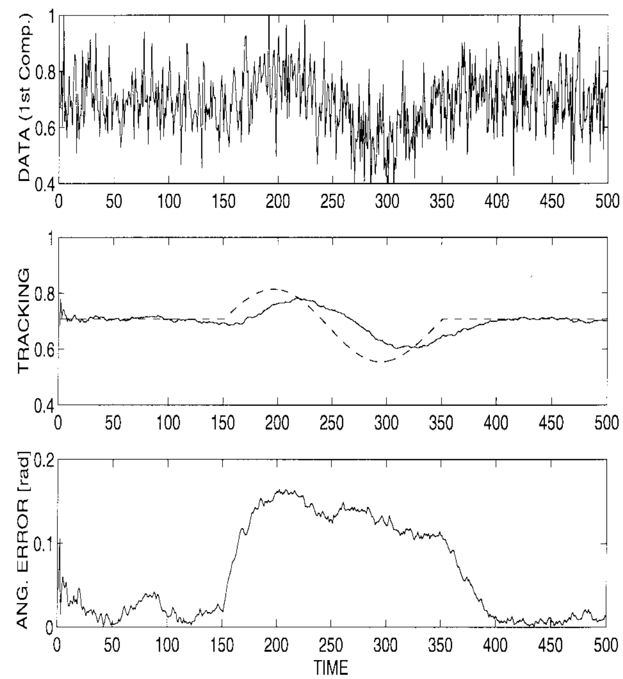

Fig. 3. Performance of the cross-product algorithm with λ =0.97. Top diagram: noisy data (first component of $\hat{z}_t$.) Middle diagram: true and estimated first component, denoted by dashed and full lines, respectively. Bottom diagram: angular estimation error.

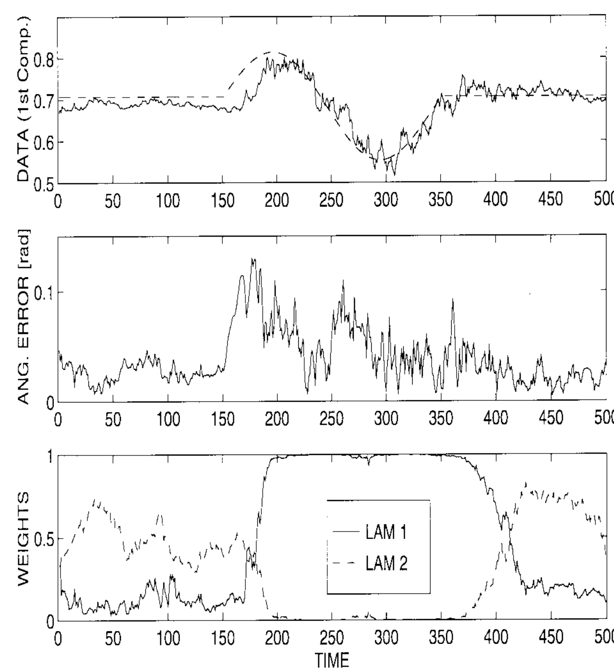

Fig. 4. Performance of the multiple forgetting factor technique. Top diagram: tracking the first data component of $\hat{z}_t$. Middle diagram: angular estimation error. Third diagram: weights of models with $\lambda = \lambda_1$ and $\lambda = \lambda_2$.

V. Concluding Remarks

We analyzed the performance of the cross-product algorithm with a forgetting factor for tracking the direction to a moving source and computed an asymptotic expression of its variance of angular estimation error. This expression was used to find the optimal forgetting factor that minimizes the error variance as a function of the source dynamics and sensor noise variances. The main advantage of this algorithm is in its computational efficiency. We then presented a more complex algorithm containing multiple forgetting factors, which has has a self tuning ability. This property is useful when no *a priori* knowledge of the source dynamics is available but requires more computations then the single cross-product algorithm. Note that both of the algorithms can be combined with a Kalman filter to improve their tracking properties in scenarios where the movement of the source is subject to a persistent drift in some direction; see [4] and [6]. We presented numerical examples demonstrating the performance of the algorithms in different scenarios.

Appendix
Analysis of the Traacking Algorithm

Recall that [2]

$$\begin{aligned}\hat{z}_t &= \text{Re}\{\boldsymbol{y}_{\text{E}}(t) \times \overline{\boldsymbol{y}}_{\text{H}}(t)\}\\ &= \boldsymbol{z}_t + \delta\boldsymbol{z}_t = \sigma_s^2\boldsymbol{u}_t + \delta\boldsymbol{z}_t, \qquad t = 0, 1, \cdots, N. \end{aligned} \tag{17}$$

It is shown that $\{\delta\boldsymbol{z}_t\}$ is a sequence of pairwise independent zero-mean random vectors. Note that the signal variance σ_s^2 may also depend on time, but in our first-order approximation, this will not affect the analysis. Further, it is assumed that the signal envelope $s(t)$ is statistically independent of $\boldsymbol{e}_{\text{E}}(t)$ and $\boldsymbol{e}_{\text{H}}(t)$ and has finite fourth-order moments.

The covariance matrix of $\delta\boldsymbol{z}_t$ is computed on the bottom of [2, p. 396]. This matrix depends on t through the instantaneous signal parameters, in particular, the vector $\boldsymbol{u}_t$ as well as the electromagnetic wave polarization. In this correspondence, we only need the following expression, which is independent of these parameters; see [2, p. 396]:

$$\begin{aligned}&\text{tr}\{(I_3 - \boldsymbol{u}_t\boldsymbol{u}_t^T)\,\text{cov}[\delta\boldsymbol{z}_t]\}\\ &\quad= \tfrac{1}{2}\,(\sigma_{\text{E}}^2 + \sigma_{\text{H}}^2)\sigma_s^2 + 2\sigma_{\text{E}}^2\sigma_{\text{H}}^2.\end{aligned} \tag{18}$$

Since for any matrices A, B with compatible dimensions, it holds that $\text{tr}(AB) = \text{tr}(BA)$ and $(I - \boldsymbol{u}_t\boldsymbol{u}_t^T)^2 = (I - \boldsymbol{u}_t\boldsymbol{u}_t^T)$; it also holds that $(I_3 - \boldsymbol{u}_t\boldsymbol{u}_t^T)^2 = (I_3 - \boldsymbol{u}_t\boldsymbol{u}_t^T)$ and that

$$\begin{aligned}&\text{tr}\{(I - \boldsymbol{u}_t\boldsymbol{u}_t^T)\,\text{cov}[\delta\boldsymbol{z}_t](I - \boldsymbol{u}_t\boldsymbol{u}_t^T)\}\\ &\quad= \tfrac{1}{2}\,(\sigma_{\text{E}}^2 + \sigma_{\text{H}}^2)\sigma_s^2 + 2\sigma_{\text{E}}^2\sigma_{\text{H}}^2.\end{aligned} \tag{19}$$

Note that the expression in (19) is the trace of the covariance matrix of $\tilde{\delta}\boldsymbol{z}_t \triangleq (I_3 - \boldsymbol{u}_t\boldsymbol{u}_t^T)\delta\boldsymbol{z}_t$. Relation (19) will be used in the sequel.

Let Δ denote the forward difference operator, e.g., $\Delta\boldsymbol{u}_t = \boldsymbol{u}_{t+1} - \boldsymbol{u}_t$, and let

$$\tilde{\Delta}\boldsymbol{u}_t = (I_3 - \boldsymbol{u}_t\boldsymbol{u}_t^T)\Delta\boldsymbol{u}_t. \tag{20}$$

For use in the later analysis, we shall derive an approximate expression for the trace of the covariance matrix of $\tilde{\Delta}\boldsymbol{u}_t$. Using the Taylor series expansion of (5), we get

$$\boldsymbol{u}_{t+1} = \boldsymbol{u}_t + [I_3 - \boldsymbol{u}_t\boldsymbol{u}_t^T]\boldsymbol{n}_t + O_{\text{UB}}(||\boldsymbol{n}_t||^2) \tag{21}$$

where $O_{\text{UB}}(||\boldsymbol{n}_t||^2)$ stands for a remainder that is uniformly bounded in norm by a constant times $||\boldsymbol{n}_t||^2$ both for all $||\boldsymbol{n}_t|| \leq 1/2$ and for all $||\boldsymbol{n}_t|| > 1/2$ (see [2, proof of Lemma H.2]). Hence

$$\begin{aligned}&\text{tr}\{\text{cov}[\tilde{\Delta}\boldsymbol{u}_t]\}\\ &\quad= \text{tr}\{\text{cov}[(I_3 - \boldsymbol{u}_t\boldsymbol{u}_t^T)\boldsymbol{n}_t]\} + \text{E}\{O_{\text{UB}}(||\boldsymbol{n}_t||^3)\}\\ &\quad= \text{tr}[(I_3 - \boldsymbol{u}_t\boldsymbol{u}_t^T)\,\text{cov}[\boldsymbol{n}_t](I_3 - \boldsymbol{u}_t\boldsymbol{u}_t^T)] + O(\sigma_n^3)\\ &\quad= \sigma_n^2\,\text{tr}(I_3 - \boldsymbol{u}_t\boldsymbol{u}_t^T) + O(\sigma_n^3) = 2\sigma_n^2 + O(\sigma_n^3).\end{aligned} \tag{22}$$

Let δ denote the estimation error operator, e.g.,

$$\delta\boldsymbol{u}_t = \hat{\boldsymbol{u}}_t - \boldsymbol{u}_t \tag{23}$$

$$\delta\boldsymbol{s}_t = \hat{\boldsymbol{s}}_t - \boldsymbol{z}_t \tag{24}$$

where we assume that $\hat{\boldsymbol{s}}_t$ in (1) is an estimate of the quantity $\boldsymbol{z}_t$ in (17) and put

$$\tilde{\delta}\boldsymbol{s}_t = (I_3 - \boldsymbol{u}_t\boldsymbol{u}_t^T)\delta\boldsymbol{s}_t. \tag{25}$$

Then, using (2), (17), and a series expansion similar to those in (5) and (21), we obtain

$$\begin{aligned}\hat{\boldsymbol{u}}_t &= \frac{\hat{\boldsymbol{s}}_t}{||\hat{\boldsymbol{s}}_t||} = \frac{\boldsymbol{z}_t + \delta\boldsymbol{s}_t}{||\boldsymbol{z}_t + \delta\boldsymbol{s}_t||} = \frac{\boldsymbol{u}_t + \delta\boldsymbol{s}_t\sigma_s^{-2}}{||\boldsymbol{u}_t + \delta\boldsymbol{s}_t\sigma_s^{-2}||}\\ &= \boldsymbol{u}_t + [I_3 - \boldsymbol{u}_t\boldsymbol{u}_t^T]\delta\boldsymbol{s}_t\sigma_s^{-2} + O_{\text{UB}}(||\delta\boldsymbol{s}_t||^2\sigma_s^{-4})\\ \delta\boldsymbol{u}_t &= \tilde{\delta}\boldsymbol{s}_t\sigma_s^{-2} + O_{\text{UB}}(||\delta\boldsymbol{s}_t||^2\sigma_s^{-4}).\end{aligned} \tag{26}$$

The angular estimation error can be approximated by

$$\begin{aligned}\delta\varphi_t &= 2\,\text{arcsin}(||\hat{\boldsymbol{u}}_t - \boldsymbol{u}_t||/2)\\ &= ||\delta\boldsymbol{u}_t|| + O_{\text{UB}}(||\delta\boldsymbol{u}_t||^3).\end{aligned} \tag{27}$$

Using (26), (27), and the fact that the absolute value of $\delta\varphi_t$ is bounded by a constant (equal to π), we get

$$\delta\varphi_t = ||\tilde{\delta}\boldsymbol{s}_t||\sigma_s^{-2} + O_{\text{UB}}(||\delta\boldsymbol{s}_t||^2\sigma_s^{-4}) \tag{28}$$

$$[\delta\varphi_t]^2 = ||\tilde{\delta}\boldsymbol{s}_t||^2\sigma_s^{-4} + O_{\text{UB}}(||\delta\boldsymbol{s}_t||^3\sigma_s^{-6}). \tag{29}$$

Hence, provided that the errors $\boldsymbol{e}_{\text{E}}$, $\boldsymbol{e}_{\text{H}}$, and $\delta\boldsymbol{s}_t$ have finite third-order moments, it holds that

$$\text{var}[\delta\varphi_t] = \text{tr}\{\text{cov}[\tilde{\delta}\boldsymbol{s}_t]\}\sigma_s^{-4} + O(\text{E}[||\tilde{\delta}\boldsymbol{s}_t||^3]\sigma_s^{-6}). \tag{30}$$

Finally, note that $\hat{\boldsymbol{s}}_t$ in (1) can be written recursively as

$$\hat{\boldsymbol{s}}_t = \lambda\hat{\boldsymbol{s}}_{t-1} + (1 - \lambda)\hat{\boldsymbol{z}}_t. \tag{31}$$

The error of $\hat{\boldsymbol{s}}_t$ is

$$\begin{aligned}\delta\boldsymbol{s}_t &= \hat{\boldsymbol{s}}_t - \boldsymbol{z}_t = \lambda\hat{\boldsymbol{s}}_{t-1} + (1 - \lambda)\hat{\boldsymbol{z}}_t - \boldsymbol{z}_t\\ &= \lambda(\boldsymbol{z}_{t-1} + \delta\boldsymbol{s}_{t-1}) + (1 - \lambda)(\boldsymbol{z}_t + \delta\boldsymbol{z}_t) - \boldsymbol{z}_t\\ &= \lambda\delta\boldsymbol{s}_{t-1} + (1 - \lambda)\delta\boldsymbol{z}_t - \lambda\Delta\boldsymbol{z}_t.\end{aligned} \tag{32}$$

Multiplying the last equality by $I_3 - \boldsymbol{u}_t\boldsymbol{u}_t^T$ and neglecting higher than first-order error terms, we get

$$\tilde{\delta}\boldsymbol{s}_t = \lambda\tilde{\delta}\boldsymbol{s}_{t-1} + (1 - \lambda)\tilde{\delta}\boldsymbol{z}_t - \lambda\tilde{\Delta}\boldsymbol{z}_t. \tag{33}$$

Thus, the error sequence $\{\tilde{\delta}\boldsymbol{s}_t\}$ can be obtained by the linear filtering of the sequencies $\{\tilde{\delta}\boldsymbol{z}_t\}$ and $\{\tilde{\Delta}\boldsymbol{z}_t\}$ in

$$\begin{aligned}\tilde{\delta}\boldsymbol{s}_t &= \frac{1 - \lambda}{1 - \lambda q^{-1}}\tilde{\delta}\boldsymbol{z}_t + \frac{-\lambda}{1 - \lambda q^{-1}}\tilde{\Delta}\boldsymbol{z}_t\\ &\triangleq \Phi_1(q^{-1})\tilde{\delta}\boldsymbol{z}_t + \Phi_2(q^{-1})\tilde{\Delta}\boldsymbol{z}_t.\end{aligned} \tag{34}$$

where q^{-1} is the backward time shift operator.

Then, in the limit $N \to \infty$, it holds that

$$\begin{aligned}&\text{tr}\{\text{cov}[\tilde{\delta}\boldsymbol{s}_t]\}\\ &\quad= \frac{1}{2\pi i}\oint \Phi_1(z)\Phi_1(z^{-1})z^{-1}\,dz \cdot \text{tr}\{\text{cov}[\tilde{\delta}\boldsymbol{z}_t]\}\\ &\qquad+ \frac{1}{2\pi i}\oint \Phi_2(z)\Phi_2(z^{-1})z^{-1}\,dz \cdot \text{tr}\{\text{cov}[\tilde{\Delta}\boldsymbol{z}_t]\}\end{aligned} \tag{35}$$

where the integration proceeds along the unit circle in the complex plane. After a straightforward calculation, we get

$$\begin{aligned}\text{tr}\{\text{cov}[\tilde{\delta}\boldsymbol{s}_t]\} &= \frac{1 - \lambda}{1 + \lambda}\,\text{tr}\{\text{cov}[\tilde{\delta}\boldsymbol{z}_t]\} + \frac{\lambda^2}{1 - \lambda^2}\\ &\quad\cdot \text{tr}\{\text{cov}[\tilde{\Delta}\boldsymbol{z}_t]\}.\end{aligned} \tag{36}$$

Now, from (17), it follows that

$$\begin{aligned}\Delta\boldsymbol{z}_t &= \boldsymbol{z}_{t+1} - \boldsymbol{z}_t = \sigma_s^2\Delta\boldsymbol{u}_t + \Delta\sigma_s^2\boldsymbol{u}_t\\ \tilde{\Delta}\boldsymbol{z}_t &= (I_3 - \boldsymbol{u}_t\boldsymbol{u}_t^T)\Delta\boldsymbol{z}_t = \sigma_s^2(I_3 - \boldsymbol{u}_t\boldsymbol{u}_t^T)\Delta\boldsymbol{u}_t\\ &= \sigma_s^2\tilde{\Delta}\boldsymbol{u}_t.\end{aligned} \tag{37}$$

and

$$\text{cov}[\tilde{\Delta}\boldsymbol{z}_t] = \sigma_s^4 \, \text{cov}[\tilde{\Delta}\boldsymbol{u}_t]. \tag{38}$$

Substituting (38), (36) and (19) into (30), we obtain (6). ■

References

[1] A. Nehorai and E. Paldi, "Vector-sensor processing for electromagnetic source localization," in *Proc. 25th Asilomar Conf. Signals, Syst. Comput.*, Pacific Grove, CA, Nov. 1991, pp. 566–572.

[2] ——, "Vector-sensor array processing for electromagnetic source localization," *IEEE Trans. Signal Processing*, vol. 42, pp. 376–398, Feb. 1994.

[3] C. M. See and A. Nehorai, "distributed electromagnetic component sensor array processing," in *Proc. 7th Workshop Adaptive Sensor Array Process.*, Lincoln Lab., Mass. Inst. Technol., Boston, MA, Mar. 1999, pp. 75–79.

[4] C. R. Rao, C. R. Sastry, and B. Zhou, "Tracking the direction of arrival of multiple moving targets," *IEEE Trans. Signal Processing*, vol. 42, pp. 1133–1143, May 1994.

[5] K. Uosaki, M. Yotsua, and T. Hatanaka, "Adaptive identification of nonstationary systems with multiple forgetting factors," in *Proc. 35th Conf. Decision Contr.*, Kobe, Japan, Dec. 1996, pp. 851–856.

[6] A. Nehorai and P. Tichavskỳ, "Cross-product algorithms for source tracking using an EM vector sensor," Rep. No. UIC-EECS-98-4, Dept. Elect. Eng. Comput. Sci., Univ. Illinois at Chicago, July 1998. Short version was presented at *ICASSP*, Phoenix, AZ, Mar. 1999, vol. 5, pp. 2781–2784.

Adaptive Multistage Beamforming Using Cyclic Higher Order Statistics (CHOS)

Massimiliano (Max) Martone

***Abstract*— A new blind beamforming algorithm for signals that exhibit higher order cyclostationarity is presented. Exploiting some recent theoretical developments, we show how cyclic cumulants of the received signals can be used to obtain the weights of the beamformer that perform blind extraction. The method is based on a spatial interpretation of a deconvolution procedure known as the super-exponential algorithm. The basic block processing algorithm is made fully adaptive using an adaptive URV scheme and applied to a typical mobile communications scenario where several cochannel inteferers corrupt the signals of interest.**

***Index Terms*—Array signal processing, higher order statistics, interference suppression, land mobile radio systems.**

I. Introduction

The use of antenna arrays in a communication system can theoretically improve performance in terms of capacity. Particularly, a multielement antenna receiver at the basestation of a cellular communication system is able to compensate signal degradations in the mobile-to-base link caused by co-channel interference, which is known to be the most important factor limiting the number of users that a system can handle. The traditional beamforming approach requires the knowledge of a "look" direction (the direction of arrival of the signal of interest) or the waveform of the signal of interest itself, which is obviously not available in the cellular environment. Several alternative solutions have been proposed in the past to solve the problem. The application of high-resolution array processing methods is not possible due to the extremely high number of wavefronts impinging over the array; the model is not identifiable. The application of subspace methods was proposed in [7], where the propagation model was considerably simplified assuming a local scattering mechanism. Blind adaptive beamforming methods appear to be more successful because no knowledge about array configuration, look direction, or desired signal is required. The most popular approach to blind beamforming is the constant modulus algorithm (CMA) array [10]. The CMA method, if basically very simple to implement, appeared to suffer from two main disadvantages: misconvergence and slow adaptation rate. Here, we propose the use of cyclic cumulants [4] to determine the set of weights that extracts the signals of interest. The method is based on the same idea introduced in [1] and [2], where the superexponential approach [3] was generalized to the multivariate model. We describe the application of the method to the space-only case in presence of cyclostationary sources and present a multistage implementation based on the architecture of [11].

This correspondence is organized as follows. In Section II, we derive the discrete time model for the communication system under analysis; in Section III, we describe the beamforming architecture, whereas the basic separating criterion to extract one of the signals is justified in Section IV. In Section V, a fully adaptive implementation is proposed, whereas in Section VI, the results of some simulations for AMPS [18], which is the current analog cellular system, are shown.

II. System Model

We assume U mobile transmitters communicating with a basestation with a K-element antenna with $U \leq K$. The structure of the antenna is assumed to be a straight line with evenly spaced elements, d is the distance between adjacent antenna elements, and $\tilde{\lambda}$ is the wavelength of the signal. The complex baseband modulated signal transmitted by the lth transmitter is $x_l(t')$. We use the notation $s(t')$ to denote a continuous time waveform, whereas we will denote $s(t)$ as the discrete-time signal obtained by sampling at equispaced instants. Due to RF multipath propagation (we will consider only the short-term fading which obeys a Rayleigh distribution), the signal received at the kth sensor of the array can be modeled as $r_k(t') = \Sigma_{l=1}^{U} \Sigma_{m=1}^{N_l} \rho_{l,m} e^{j\psi_{l,m}} a_k(\theta_{l,m}) x_l(t') + \eta_k(t')$, where

N_l	number of paths relative to the scattering model of the lth transmitter[1]
$\rho_{l,m}$	Rayleigh distributed random variable;
$\psi_{l,m}$	uniformly distributed over $[0, 2\pi]$;
$a_k(\theta_{l,m})$	unknown gain and phase response of the kth sensor in the angle of arrival $\theta_{l,m}$;
$\eta_k(t')$	noise at the kth sensor.

If the sources can be considered narrowband, then $a_k(\theta_{l,m}) = e^{-j(n-1)2\pi(d/\tilde{\lambda})\, sin\, \theta_{l,m}}$. It is important to observe that the application of the algorithm described in the following is not limited to this array configuration (the uniform linear array case). Sampling at

[1] It is important to observe that each discrete path is a linear combination of a large number of unresolved paths that justifies the complex Gaussian assumption for $\xi_{l,m} = \rho_{l,m} e^{j\psi_{l,m}}$

Manuscript received April 30, 1997; revised March 26, 1999. The associate editor coordinating the review of this paper and approving it for publication was Dr. Jonathon A. Chambers.

The author is with the Telecommunications Group 700, Watkins-Johnson Company, Gaithersburg, MD 20878-1794 USA.

Publisher Item Identifier S 1053-587X(99)07663-1.